ATMOSPHERIC SCIENCE LETTERS
Atmos. Sci. Let. (2015)
Published online in Wiley Online Library
(wileyonlinelibrary.com) **DOI:** 10.1002/asl.635

RMetS
Royal Meteorological Society

Land surface–atmosphere interaction in future South American climate using a multi-model ensemble

R. C. Ruscica,[1] C. G. Menéndez[1,2] and A. A. Sörensson[1]*

[1]*Centro de Investigaciones del Mar y la Atmósfera, Consejo Nacional de Investigaciones Científicas y Técnicas, Universidad de Buenos Aires, Argentina*
[2]*Departamento de Ciencias de la Atmósfera y los Océanos, FCEN, Universidad de Buenos Aires, Argentina*

**Correspondence to:*
A. A. Sörensson, Centro de Investigaciones del Mar y la Atmósfera, Consejo Nacional de Investigaciones Científicas y Técnicas, Universidad de Buenos Aires, Ciudad Universitaria, Int. Guiraldes 2160, Pabellón 2, Piso 2, Ciudad Autónoma de Buenos Aires C1428EGA, Argentina.
E-mail: sorensson@cima.fcen.uba.ar

Received: 7 June 2015
Revised: 12 August 2015
Accepted: 13 October 2015

Abstract

The land–atmosphere interaction for reference and future climate is estimated with a regional climate model ensemble. In reference climate, more than 50% of the models show interaction in southeastern South America during austral spring, summer and autumn. In future climate, the region remains a strong hotspot although somewhat weakened due to the wet response that enhance energy limitation on the evapotranspiration. The region of the Brazilian Highlands and Matto Grosso appears as a new extensive hotspot during austral spring. This is related to a dry response which is probably accentuated by land surface feedbacks.

Keywords: land–atmosphere interaction; soil moisture; precipitation; coupling; South America; regional climate modeling

1. Introduction

On a monthly to seasonal time scale, soil moisture (SM) has potential to be a low-frequency modulator of climate because of its influence on the partitioning of heat fluxes and its long memory (e.g. Eltahir, 1998). Therefore, forecasts could be improved by including estimates of SM for the regions and seasons where this variable exerts a control on the atmosphere.

For SM to control precipitation (PP), the evapotranspiration (ET) regime has to be limited by SM rather than by radiation. The radiation (or energy)-limited ET regime dominates in wet regions where the moisture stress is low and variability of SM does not affect ET. In dry climates, SM availability is a first-order constraint on ET (e.g. Koster *et al.*, 2004), but in very dry areas, however, SM does not affect PP because ET variability is too weak to induce PP generation. Therefore, regions where SM exerts control on PP tend to appear over transitions zones between dry and wet climates (Koster *et al.*, 2004). A changing climate could alter these regimes due to increasing temperatures and altered PP amounts and temporal distribution.

South America embraces vast areas of both SM-limited regions, such as the Patagonian semi-arid steppe, and energy-limited regions, such as the Amazon rainforest. Southeastern South America (SESA) is one of the regions that have been identified as SM limited (Jung *et al.*, 2010). SESA has also been identified as a region with strong SM–ET and SM–PP coupling during austral summer (DJF) in climate model studies (Wang *et al.*, 2007; Sörensson and Menéndez, 2011; Dirmeyer *et al.*, 2012; Ruscica *et al.*, 2015) and as a region of SM–ET coupling during austral autumn (MAM) and spring (SON, Ruscica *et al.*, 2015). In a reanalysis study by Zeng *et al.* (2010), subtropical South America was found to be a hotspot of interaction between SM and PP for DJF. Somewhat contrasting to these results, Dirmeyer *et al.* (2009) used data from several land surface models and identified SESA and the southern Amazon basin in boreal summer (JJA) as well as northeastern Brazil (NeB) and the Altiplano in MAM as regions that combine both land–atmosphere interactions and memory longer than 2 weeks, i.e. regions where forecasts could be improved by including SM information. On the other hand, a great number of studies on the global scale has focused on JJA (Koster *et al.*, 2004; Notaro, 2008; Orlowsky and Seneviratne, 2010; Wei and Dirmeyer, 2010; Zeng *et al.*, 2010; Zhang *et al.*, 2011), showing different locations of high interaction in the South American tropics and agreeing on the absence of SM–ET and SM–PP interactions in subtropical areas.

The purpose of this work is to identify regions of land–atmosphere interaction over South America for all seasons and to identify changes in location and strength of these hotspots in future climate. The study is original in the sense that we use an ensemble of regional climate models (RCMs) simulations, which enhances the spatial resolution in comparison with global climate model (GCM) studies and spans a wider range of uncertainty than single-model studies.

Table 1. Basic information on the ensemble members.

	RCA	RegCM3	PROMES	LMDZ
GCM forcing at lateral boundaries and SST	EC5OM-R1, EC5OM-R2 and EC5OM-R3 (Roeckner *et al.*, 2006)	EC5OM-R1 and HadCM3-Q0 (Gordon *et al.*, 2000)	HadCM3-Q0	EC5OM-R3 and IPSL (Hourdin *et al.*, 2006)
Reference	Samuelsson *et al.* (2011)	da Rocha *et al.* (2009)	Domínguez *et al.* (2010)	Hourdin *et al.* (2006)
Number of vertical atmospheric levels	40	18	37	19
Number of soil moisture levels	2	2	2	2

2. Models and methodology

The CLARIS-LPB project (Boulanger *et al.*, 2011) has provided the first coordinated ensemble of RCM climate change simulations over the South American continent. The ensemble, which covers the period 1961–2100, is designed to span uncertainty of climate change scenarios using several RCMs forced by lateral boundary conditions and sea surface temperature from different GCMs, for the emission scenario A1B (Sánchez *et al.*, 2015). In this study, we use time series of seasonal values of ET and PP for a period of 30 years of reference climate (1961–1990) and future climate (2071–2100) of eight ensemble members based on the combinations of four RCMs forced by three GCMs (Table 1). The land surface schemes of all four RCMs are second generation schemes where stomatal control on ET is parameterized (Sellers *et al.*, 1997). The domains differ slightly among the models due to different types of grids, but all are of continental scale with borders over the surrounding oceans and a horizontal resolution of $0.5° \times 0.5°$. All models are hydrostatic.

The regions of SM–PP interaction are estimated with the index Γ, described by Zeng *et al.* (2010). Γ is defined as:

$$\Gamma = r_{pp,ET} \cdot \frac{\sigma_{\mathrm{ET}}}{\sigma_{\mathrm{PP}}}$$

where $r_{\mathrm{PP,ET}}$ is the correlation between the time series of seasonal means of PP and ET, and the standard deviations σ_{ET} and σ_{PP} represent their temporal variability. For regions and seasons where the runoff is small in comparison to infiltration, PP can be interpreted as a proxy for SM. If $r_{\mathrm{PP,ET}}$ is positive (negative), ET is SM (energy) limited. A necessary, although not sufficient, condition for SM to influence on PP is that the variability of ET is high enough. This criterion surges since, over dry regions, although ET is controlled by SM, the ET anomaly generated by a SM anomaly could be too small to generate a PP anomaly (Guo *et al.*, 2006). In the Γ index, this criterion is represented by the variability of ET normalized by the variability of PP. To avoid spuriously high values of Γ, regions where interannual rainfall variability for each season is less than $0.5\,\mathrm{mm\,day^{-1}}$ are not included in the analysis.

3. Results

The observed and ensemble seasonal mean PP for the reference period are shown in Figure 1(a)–(d) (CRU TS3.1, Mitchell and Jones, 2005) and Figure 1(e)–(h), respectively. In the northeastern corner of Brazil during DJF, the ensemble simulates rainfall of $8\,\mathrm{mm\,day^{-1}}$ in a semiarid region of $1–2\,\mathrm{mm\,day^{-1}}$. This bias is the result of an artifact of the driving GCMs which, instead of the intertropical and the South Atlantic convergence zones, simulate only one convergence zone, with a maximum over this very dry region (Lin, 2007). When the RCMs of the ensemble are driven by reanalysis (Solman *et al.*, 2013), this bias is not present. In SESA, there is an underestimation of rainfall for all seasons. This dry bias is common in both GCMs and RCMs (Vera *et al.*, 2006; Menéndez *et al.*, 2010) and is also present when the RCMs of the ensemble are driven by reanalysis (Solman *et al.*, 2013).

The ensemble ET is shown in Figure 1(i)–(l). The spatial pattern resembles that of the PP with maximum located approximately over the same regions, except for in very wet situations such as in DJF over central Brazil or in JJA north of the equator. Over dry regions, the magnitude of the two variables is similar, while in wet regions such as the Amazonia, more than half of the PP goes to runoff.

The ensemble mean response to climate change is shown in Figure 2. The response of PP (Figure 2(a)–(d)) shows a dipole pattern of wet response over SESA and dry response north of it, similar to the study by Dirmeyer *et al.* (2014). Over SESA, future PP increases in DJF, MAM and SON with up to $1\,\mathrm{mm\,day^{-1}}$ (10–30% of reference PP), and around the border between Argentina, Paraguay and Brazil in SON, the response is larger than $1\,\mathrm{mm\,day^{-1}}$. The dry response is strongest in SON and extends over the entire continent north of 20°S. Figure 2(e)–(h) shows that the mean ET response has a similar pattern, although of less magnitude and extension. Over permanent wet regions such as the western Amazon basin or southern Chile, the mean PP decreases without any remarkable changes in mean ET, leading to potential decreased river discharge, similar to the results by Pokhrel *et al.* (2014) and Dirmeyer *et al.* (2014). Worth to notice is that even though the annual temperature of the Amazon region increases with 3°–6° (Sánchez *et al.*, 2015), which

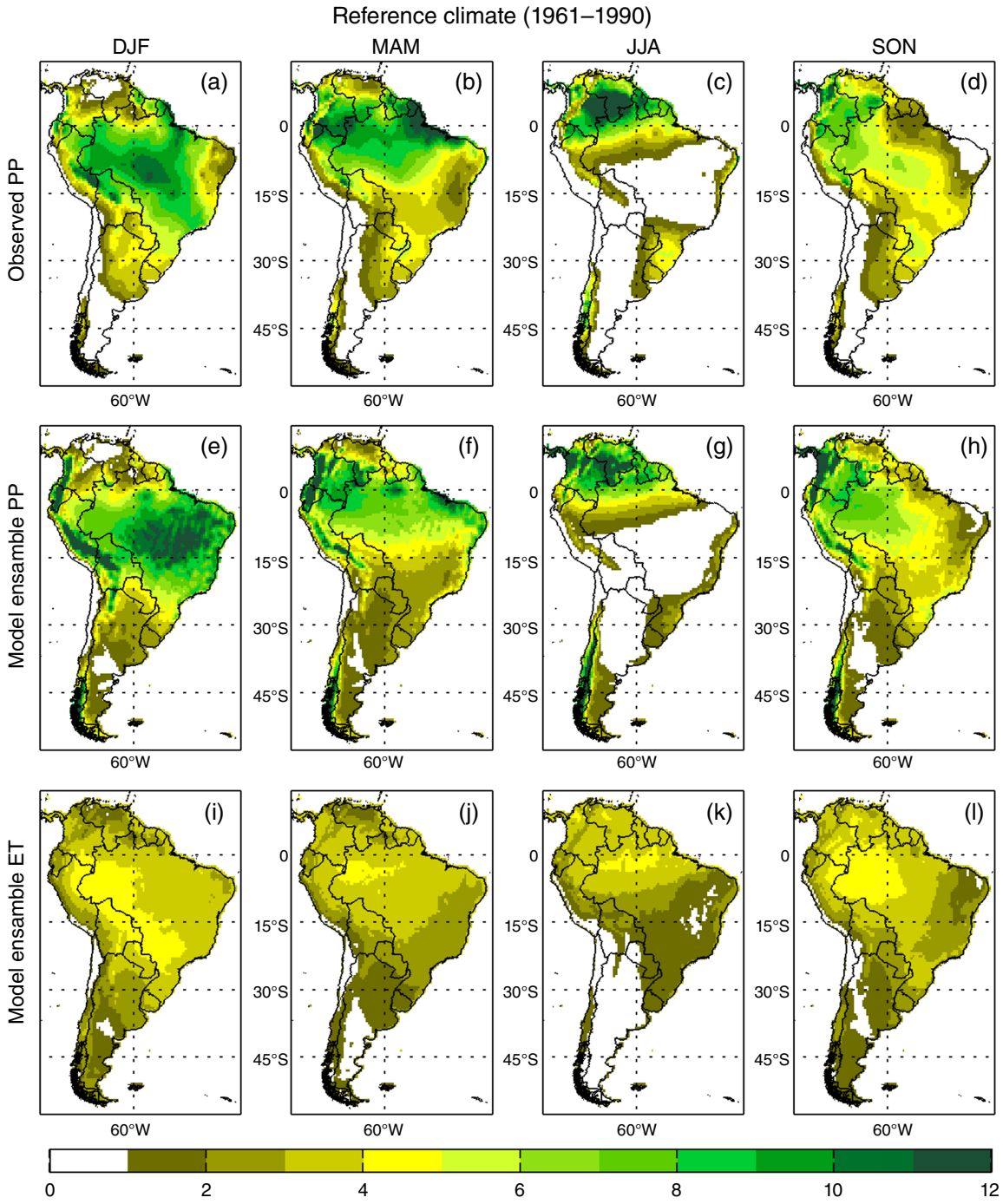

Figure 1. Seasonal means of continental precipitation (PP) and evapotranspiration (ET) during austral summer (DJF), autumn (MAM), winter (JJA) and spring (SON) in the reference climate period (1961–1990). Upper panels (a)–(d): observed PP of the CRU database. Middle panels (e)–(h): ensemble mean PP. Lower panels (i)–(l): ensemble mean ET. Units: mm day^{-1}.

should increase atmospheric demand, the ET does not increase. This could be due to other factors such as decreased wind speed, less insolation due to more clouds or stomata closure due to high temperatures.

Consensus results of land–atmosphere interaction were localized by calculating the number of ensemble members that had a Γ index equal or higher than 0.25. This is shown for the reference climate in Figure 3(a)–(d). There is a clear agreement among members that SESA is a region of land–atmosphere interaction (hotspot) for all seasons, except JJA. The hotspot is strongest in DJF, where it extends from northern Patagonia in the south to Paraguay in the north and includes Uruguay and southern Brazil. In MAM and SON, the level of inter-member agreement is lower than in DJF, and the hotspot is located more inlands and further north. Overall, this is consistent with Wang *et al.* (2007); Sörensson and Menéndez (2011) and Ruscica *et al.* (2015). In SON, more than 50% of the ensemble members agree on land–atmosphere interaction over NeB. This is reasonable because during the dry JJA (Figure 1(g)), the soil water is depleted over this region,

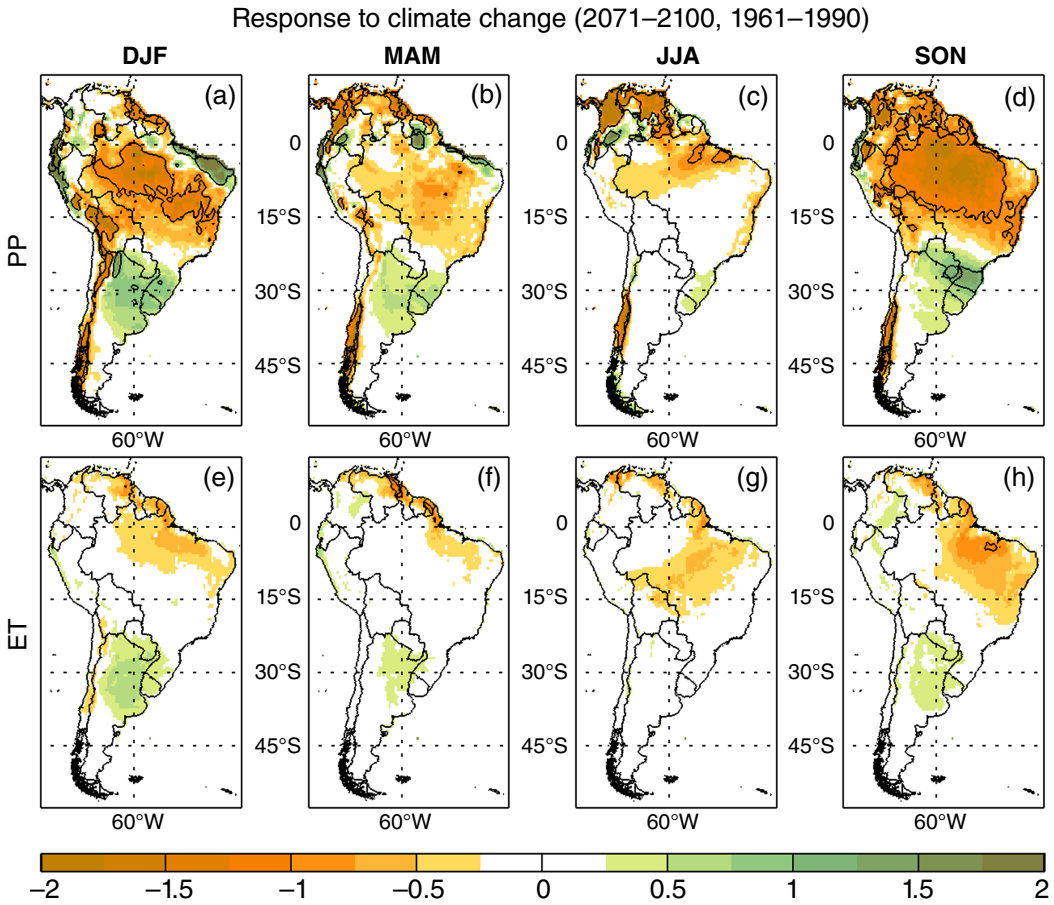

Figure 2. Ensemble response to climate change, defined as the difference of the future and reference climate mean fields (2071–2100 minus 1961–1990). Upper panels (a)–(d): precipitation (PP). Lower panels (e)–(h): evapotranspiration (ET). Units: mm day^{-1}. Contour lines delimit regions with a climate response of more (less) than 1 mm day^{-1} (−1 mm day^{-1}).

and when the wet season starts in SON (Figure 1(h)), the SM responds to the PP and ET responds to SM. It should be recalled that the very eastern corner of NeB has a wet PP bias in SON due to the GCM forcing (Figure 1(d) and (h)). During the same season, SON, half of the members show land–atmosphere interaction over eastern Amazonia.

Figure 3(e)–(h) summarizes the size and location of the hotspots in both periods of analysis. In future climate, SESA is still a region of high interaction (orange zones). This result is similar to the study by Dirmeyer *et al.* (2012), who analyzed the land–atmosphere interaction with a very high-resolution GCM for DJF and JJA for present and future climate. The most notable response to climate change (violet zones) on the continental scale occurs over the Brazilian Highlands and Matto Grosso, where many members agree on strong interaction during SON. This is a consequence of the dryer future climate during this season (Figure 2(h)), transforming the region in a transition zone with better potential conditions for the SM–PP coupling. Over the eastern corner of NeB, the hotspot is lost (green zone) in future climate. This is because Γ is not defined for regions where PP variability is less than 0.5 mm day^{-1}, and this region loses variability as the mean value decreases (Figure 2(d)). Over the Amazon region in JJA, it can be seen how the double dry–wet transition zone line (green and orange grid points) migrates to a northern single one (violet grid points). This is consistent with the northward shift of the maximum PP gradient during this season (see Figures 1(g) and 2(c)). Central and eastern Amazonia maintain their energy-limited ET regime in spite of decreased PP (Figure 2(a)–(d)), which is in agreement with the Pokhrel *et al.* (2014) study that drive a land hydrology model with future scenario from a GCM.

As SESA in DJF is the most important and well-defined hotspot on the continental scale in both climates, Figure 4 summarizes the response of its size and strength over this region. The red region in the Buenos Aires province is a region where seven to eight members agree on interaction in both reference and future climate (strong hotspot). The violet color over northeastern Argentina and Uruguay and the dark blue over southern Brazil mark regions where the land–atmosphere interaction loses in importance. This is the region of strongest wet response in SESA (Figure 2(a)), and as the PP response is higher than the ET response, the SM should also be higher in the future, being coherent with more energy-limited regime. The green color of the periphery of the hotspot is a moderate hotspot in both climates. This region has

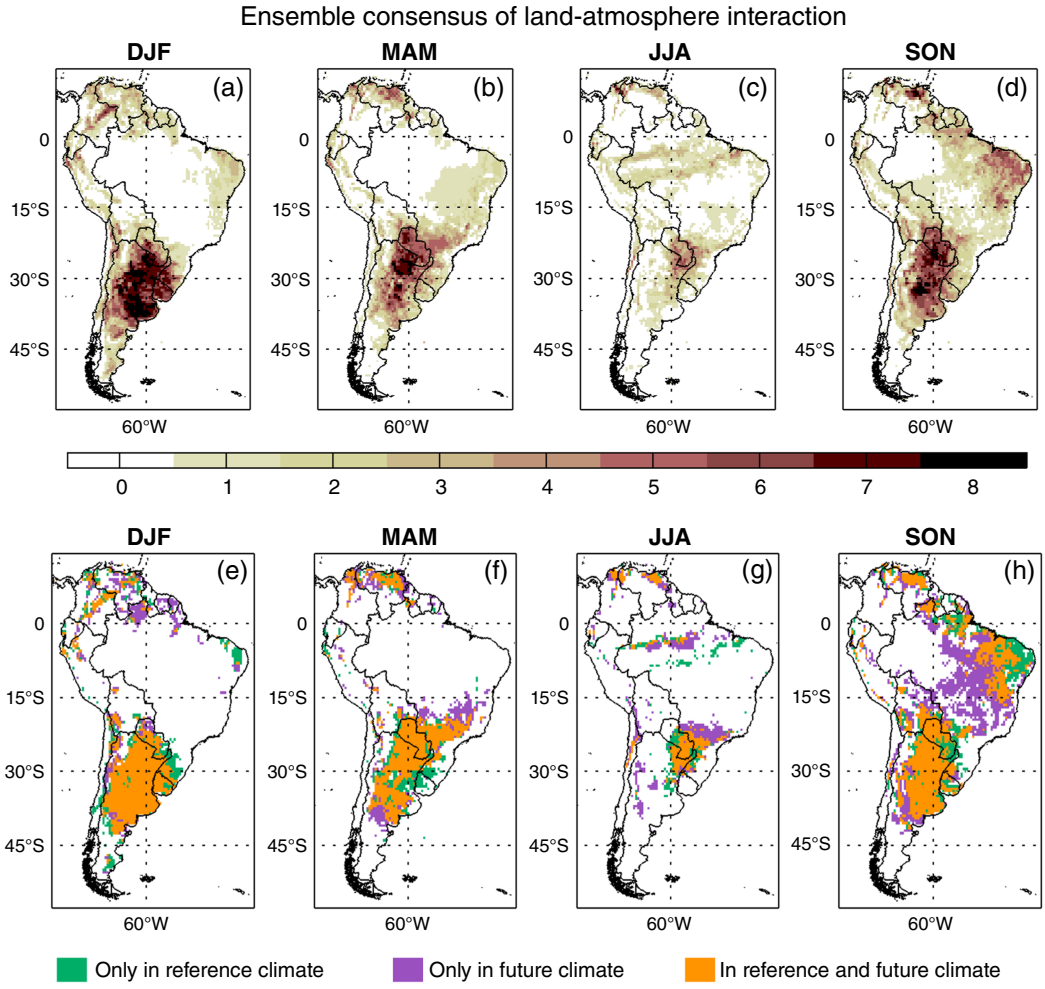

Figure 3. Upper panels (a)–(d): number of ensemble members with land–atmosphere interaction in the reference climate (1961–1990). White land grid points indicate regions without interaction or regions where Γ is not defined (see text for detailed description). Lower panels (e)–(h): extension and location of hotspots of land–atmosphere interaction that exist only in reference climate (1961–1990, green), only in future climate (2071–2100, violet) and that coexist in both climate periods (orange). Hotspot is defined as a region where three or more ensemble members coincide on having land–atmosphere interaction. White continental grid points indicate regions without hotspots in neither period.

a mean response of PP and ET of similar magnitude [less than 0.25 mm day^{-1}, Figure 2(a) and (e)], which is consistent with that the level of SM limitation does not change in the future.

4. Discussion and conclusions

The objectives of this study were to (1) achieve an estimation of land–atmosphere interaction over South America for all seasons and (2) evaluate the response of the interaction to future climate. For this purpose, an index representing land–atmosphere interaction was evaluated for an ensemble of eight RCM–GCM members for both reference and future climate.

The Γ index is advantageous in comparison with others since it is easily computed, does not require ad hoc experiments with climate models and can be used for any consistent ET and PP datasets. However, its main disadvantage is that it does not isolate the causality between two variables (e.g. SM anomalies and PP anomalies). High Γ values identify regions where land–atmosphere interactions are possible and likely, but, a high correlation between two variables could also be caused by a third one, i.e. a common forcing as SST (Orlowsky and Seneviratne, 2010). However, the results obtained here agree with other modeling studies whose methodologies isolate SM variability as a cause of ET and PP variabilities (Wang *et al.*, 2007; Sörensson and Menéndez, 2011; Ruscica *et al.*, 2014, 2015).

For reference climate (1961–1990), SESA appears as a region of strong land–atmosphere interaction, in particular during austral summer (DJF). This is consistent with other studies (Sörensson and Menéndez, 2011; Dirmeyer *et al.*, 2012; Ruscica *et al.*, 2015), where the most robust hotspot is found during DJF when the variability of ET is high enough to get an effective land–atmosphere interaction. In austral winter (JJA), which is the coldest and driest season in SESA, the region of interaction has a smaller extension and there is less coincidence among ensemble members. However, SESA is simulated too dry in most ensemble

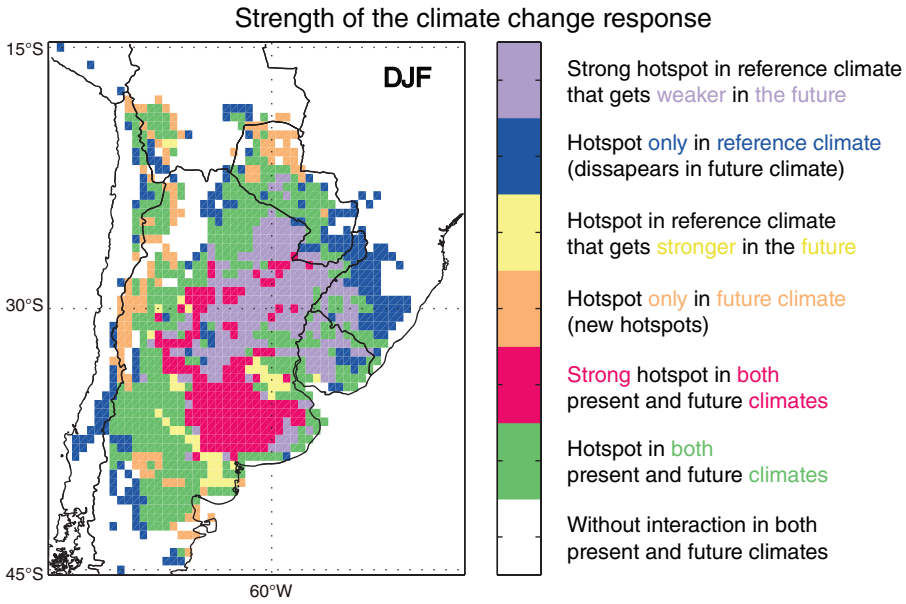

Figure 4. Response of extension and strength of the hotspot over SESA and surroundings in DJF. The definition of hotspot is the same as in Figure 3(e)–(h), and strong hotspot is defined as the agreement of seven to eight ensemble members.

members/seasons, which probably will accentuate the interaction (Ruscica *et al.*, 2015).

More than half of the members agree on strong interaction over NeB and eastern Amazonia during austral spring (SON). In DJF and austral autumn (MAM), the ensemble has a large wet bias over NeB, and therefore it is possible that this region has a strong interaction also in these seasons without being captured by this ensemble.

In future climate, SESA maintains its status as a hotspot, with in general less agreement between members. In regions where PP increases more than ET in DJF, the hotspot loses in strength and extension, while in regions where the response of the two variables is similar, the hotspot maintains its strength. This could be explained by the fact that in the latter case, the region maintains the same level of SM limitation, while in the first case, the ET depends more on atmospheric demand in future climate. In SON, the Brazilian Highlands and Matto Grosso appear as a new, extensive hotspot. This is due to the strong negative response of PP and ET, converting the energy-limited region to a SM-limited region. The dry trend over this region is consistent with the single model results by Sörensson *et al.* (2010). They found that the dry response of SON is associated with a longer dry season in this region and a delay of the monsoon onset. The results here are important because they suggest that this trend can in part be due to, or be amplified by, positive land–atmosphere feedbacks.

Acknowledgements

We acknowledge the European Community's Seventh Framework Program (CLARIS-LPB, Grant Agreement No 212492) and projects LEFE/INSU AO2015-876370 (CNRS, France), PIP No 11220110100932 (CONICET, Argentina) and PICT 2014-0887 (ANPCyT, Argentina).

References

Boulanger JP, Schlindwein S, Gentile E. 2011. CLARIS LPB WP1: metamorphosis of the CLARIS LPB European project: from a mechanistic to a systemic approach. *CLIVAR Exchanges* **16–57**: 7–10.

Dirmeyer PA, Schlosser CA, Brubaker KL. 2009. Precipitation, recycling, and land memory: an integrated analysis. *Journal of Hydrometeorology* **10**: 278–288, doi: 10.1175/2008JHM1016.1.

Dirmeyer PA, Cash BA, Kinter III JL, Stan C, Jung T, Marx L, Towers P, Wedi N, Adams JM, Altshuler EL, Huang B, Jin EK, Manganello J. 2012. Evidence for enhanced land–atmosphere feedback in a warming climate. *Journal of Hydrometeorology* **13**: 981–995, doi: 10.1175/JHM-D-11-0104.1.

Dirmeyer PA, Fang G, Wang Z, Yadav P, Milton A. 2014. Climate change and sectors of the surface water cycle in CMIP5 projections. *Hydrology and Earth System Sciences* **18**: 5317–5329, doi: 10.5194/hess-18-5317-2014.

Domínguez M, Gaertner MA, de Rosnay P, Losada T. 2010. A regional climate model simulation over West Africa: parameterization tests and analysis of land-surface fields. *Climate Dynamics* **35**: 249–265, doi: 10.1007/s00382-010-0769-3.

Eltahir EAB. 1998. A soil moisture-rainfall feedback mechanism. 1.Theory and observations. *Water Resources Research* **34**: 765–776.

Gordon C, Cooper C, Senior CA, Banks H, Gregory JM, Johns TC, Mitchell JFB, Wood RA. 2000. The simulation of SST, sea ice extents and ocean heat transports in a version of the Hadley Centre coupled model without flux adjustments. *Climate Dynamics* **16**: 147–168, doi: 10.1007/s003820050010.

Guo Z, Dirmeyer PA, Koster RD, Sud YC, Bonan G, Oleson KW, Chan E, Verseghy D, Cox P, Gordon CT, McGregor JL, Kanae S, Kowalczyk E, Lawrence D, Liu P, Mocko D, Lu C-H, Mitchell K, Malyshev S, McAvaney B, Oki T, Yamada T, Pitman A, Taylor CM, Vasic R, Xue Y. 2006. GLACE: the global land–atmosphere coupling experiment. Part II: analysis. *Journal of Hydrometeorology* **7**: 611–625, doi: 10.1175/JHM511.1.

Hourdin F, Musat I, Bony S, Braconnot P, Codron F, Dufresne J-L, Fairhead L, Filiberti M-A, Friedlingstein P, Grandpeix J-Y, Krinner K, LeVan P, Li Z-X, Lott F. 2006. The LMDZ4 general circulation model: climate performance and sensitivity to parametrized physics with emphasis on tropical convection. *Climate Dynamics* **27**: 787–813, doi: 10.1007/s00382-006-0158-0.

Jung M, Reichstein M, Ciais P, Seneviratne SI, Sheffield J, Goulden ML, Bonan G, Cescatti A, Chen J, de Jeu R, Dolman JA, Eugster W,

Gerten D, Gianelle D, Gobron N, Heinke J, Kimball J, Law BE, Montagnani L, Mu Q, Mueller B, Oleson K, Papale D, Richardson AD, Roupsard O, Running S, Tomelleri E, Viovy N, Weber U, Williams C, Wood E, Zaehle S, Zhang K. 2010. Recent decline in the global land evapotranspiration trend due to limited moisture supply. *Nature* **467**: 951–954, doi: 10.1038/nature09396.

Koster RD, Dirmeyer PA, Guo Z, Bonan G, Chan E, Cox P, Gordon CT, Kanae S, Kowalczyk E, Lawrence D, Liu P, Lu C-H, Malyshev S, McAvaney B, Mitchell K, Mocko D, Oki T, Oleson K, Pitman A, Sud YC, Taylor CM, Verseghy D, Vasic R, Xue Y, Yamada T. 2004. Regions of coupling between soil moisture and precipitation. *Science* **305**: 1138–1140, doi: 10.1126/science.1100217.

Lin JL. 2007. The double-ITCZ problem in IPCC AR4 coupled GCMs: ocean–atmosphere feedback analysis. *Journal of Climate* **20**: 4497–4525, doi: 10.1175/JCLI4272.1.

Menéndez CG, de Castro M, Boulanger J-P, D'Onofrio A, Sanchez E, Sörensson AA, Blazquez J, Elizalde A, Jacob D, Le Treut H, Li ZX, Núñez MN, Pessacg N, Pfeiffer S, Rojas M, Rolla A, Samuelsson P, Solman SA, Teichmann C. 2010. Downscaling extreme month-long anomalies in southern South America. *Climatic Change* **98**: 379–403, doi: 10.1007/s10584-009-9739-3.

Mitchell TD, Jones PD. 2005. An improved method of constructing a database of monthly climate observations and associated high resolution grids. *International Journal of Climatology* **25**: 693–712, doi: 10.1002/joc.118.

Notaro M. 2008. Statistical identification of global hot spots in soil moisture feedbacks among IPCC AR4 models. *Journal of Geophysical Research* **113**: D09101, doi: 10.1029/2007JD009199.

Orlowsky B, Seneviratne SI. 2010. Statistical analyses of land atmosphere feedbacks and their possible pitfalls. *Journal of Climate* **23**: 3918–3932, doi: 10.1175/2010JCLI3366.

Pokhrel YN, Fan Y, Miguez-Macho G. 2014. Potential hydrologic changes in the Amazon by the end of the 21st century and the groundwater buffer. *Environmental Research Letters* **9**: 084004, doi: 10.1088/1748-9326/9/8/084004.

Roeckner E, Brokopf R, Esch M, Giorgetta M, Hagemann S, Kornblueh L, Manzini E, Schlese U, Schulzweida U. 2006. Sensitivity of simulated climate to horizontal and vertical resolution in the ECHAM5 atmosphere model. *Journal of Climate* **19**: 3771–3791, doi: 10.1175/JCLI3824.1.

Ruscica RC, Sörensson AA, Menéndez CG. 2014. Hydrological links in southeastern South America: soil moisture memory and coupling within a hot spot. *International Journal of Climatology* **34**: 3641–3653, doi: 10.1002/joc.3930.

Ruscica RC, Sörensson AA, Menéndez CG. 2015. Pathways between soil moisture and precipitation in southeastern South America. *Atmospheric Science Letters* **16**: 267–272, doi: 10.1002/asl2.552.

Samuelsson P, Jones CG, Willén U, Ullerstig A, Gollvik S, Hansson U, Jansson C, Kjellström E, Nikulin G, Wyser K. 2011. The Rossby centre regional climate model RCA3: model description and performance. *Tellus A* **63**: 4–23, doi: 10.1111/j.1600-0870.2010.00478.x.

Sánchez E, Solman S, Remedio ARC, Berbery H, Samuelsson P, Da Rocha RP, Mourão C, Li L, Marengo J, de Castro M, Jacob D. 2015. Regional climate modelling in CLARIS-LPB: a concerted approach towards twentyfirst century projections of regional temperature and precipitation over South America. *Climate Dynamics* **45**: 2193–2212, doi: 10.1007/s00382-014-2466-0.

Sellers PJ, Dickinson RE, Randall DA, Betts AK, Hall FG, Berry JA, Collatz GJ, Denning AS, Mooney HA, Nobre CA, Sato N, Field CB, Henderson-Sellers A. 1997. Modeling the exchanges of energy, water, and carbon between continents and the atmosphere. *Science* **275**(5299): 502–509, doi: 10.1126/science.275.5299.502.

Solman SA, Sanchez E, Samuelsson P, da Rocha RP, Li L, Marengo J, Pessacg NL, Remedio ARC, Chou SC, Berbery H, Le Treut H, de Castro M, Jacob D. 2013. Evaluation of an ensemble of regional climate model simulations over South America driven by the ERA-interim reanalysis: model performance and uncertainties. *Climate Dynamics* **41**: 1139–1159, doi: 10.1007/s00382-013-1667-2.

Sörensson AA, Menéndez CG. 2011. Summer soil-precipitation coupling in South America. *Tellus A* **63**: 56–68, doi: 10.1111/j.1600-0870.2010.00468.x.

Sörensson AA, Menéndez CG, Ruscica R, Alexander P, Samuelsson P, Willén U. 2010. Projected precipitation changes in South America: a dynamical downscaling within CLARIS. *Meteorologische Zeitschrift* **19**: 347–355, doi: 10.1127/0941-2948/2010/0467.

Vera C, Silvestri G, Liebmann B, Gonzalez P. 2006. Climate change scenarios for seasonal precipitation in South America from IPCC-AR4 models. *Geophysical Research Letters* **33**: L13707, doi: 10.1029/2006GL025759.

Wang G, Yeonjoo K, Wang D. 2007. Quantifying the strength of soil moisture–precipitation coupling and its sensitivity to changes in surface water budget. *Journal of Hydrometeorology* **8**: 551–570, doi: 10.1175/JHM573.1.

Wei J, Dirmeyer PA. 2010. Toward understanding the large-scale land-atmosphere coupling in the models: roles of different processes. *Geophysical Research Letters* **37**: L19707, doi: 10.1029/2010GL044769.

Zeng X, Barlage M, Castro C, Fling K. 2010. Comparison of land–precipitation coupling strength using observations and models. *Journal of Hydrometeorology* **11**: 979–994, doi: 10.1175/2010JHM1226.1.

Zhang L, Dirmeyer PA, Wei J, Guo Z, Cheng-Hsuan L. 2011. Land–atmosphere coupling strength in the global forecast system. *Journal of Hydrometeorology* **12**: 147–156, doi: 10.1175/2010JHM1319.1.